PROCEEDINGS OF SCIENCE

Unfolding the Muon Neutrino Spectrum with Eleven Years of IceCube Data

The IceCube Collaboration
(a complete list of authors can be found at the end of the proceedings)

E-mail: lene.vanrootselaar@tu-dortmund.de

The IceCube Neutrino Observatory, a cubic-kilometre detector embedded in the glacial ice of the South Pole, is designed to detect neutrinos across a broad energy range, from a few GeV to several PeV. This enables precise measurements of the neutrino energy spectrum, comprising the diffuse astrophysical flux, the conventional atmospheric flux from pion and kaon decays, and the not yet detected prompt neutrino flux from charmed hadron decays. Investigating the prompt component, expected to dominate in the crossover region between the other two, is a critical focus for understanding neutrino interactions, atmospheric processes, and cosmic ray composition.
This analysis determines the muon neutrino energy spectrum in the sensitive energy range between 500 GeV and 4 PeV with eleven years of IceCube data. We used an unfolding technique, which allows for model-independent determination and re-bins the observable space to ensure sufficient statistics at the highest energies. In addition to improving the precision of intermediate-energy spectral measurements, it provides the first reconstruction of the muon neutrino flux across five zenith angle bins from 86° to 180°, increasing IceCube's energy range and enabling comparisons with theoretical models and prior measurements.

Corresponding authors: Lene van Rootselaar[1*]
[1] *TU Dortmund, Otto-Hahn-Straße 4a, Dortmund, Germany*
[*] Presenter

39th International Cosmic Ray Conference (ICRC2025)
15–24 July 2025
Geneva, Switzerland

PoS(ICRC2025)1199

1. Introduction

IceCube is a cubic-kilometer neutrino detector located at the South Pole, designed to observe high-energy neutrinos from astrophysical and atmospheric sources. Neutrinos are valuable messengers in astroparticle physics, traversing cosmic distances with minimal interaction. They exist in three flavors—electron, muon, and tau—whose relative abundances across energies remain an active research area [1]. Muon neutrinos are the most commonly observed in IceCube because their charged-current interactions produce track-like signatures. Muons have relatively high masses and long lifetimes, allowing them to travel far through the detector. This makes muon neutrinos easier to identify than electron or tau neutrinos, and therefore well suited for flux measurements.

Measuring the muon neutrino spectrum also offers insights into cosmic ray interactions and the resulting atmospheric neutrino production. When high-energy cosmic rays strike the Earth's atmosphere, they initiate air showers, producing mesons such as pions and kaons, which decay into muons and neutrinos. The resulting atmospheric neutrino flux depends on both the primary cosmic ray spectrum and composition, as well as the hadronic interaction processes involved. Studying the energy and angular distribution of these neutrinos therefore contributes to more precise modeling of hadronic processes in the atmosphere and helps constrain the background for astrophysical neutrino observations and other rare event searches. In addition, the measured spectrum can complement direct searches for diffuse astrophysical flux [2]. This paper presents a measurement of the muon neutrino spectrum using 11 years of IceCube data, with particular focus on its angular dependence.

2. Angular Dependence of the Muon Neutrino Flux

The observed muon neutrino flux consists of three components: conventional and prompt atmospheric fluxes, and the astrophysical flux. Conventional and prompt neutrinos originate from cosmic-ray-induced air showers in the Earth's atmosphere. The conventional flux arises primarily from the decay of light mesons such as pions and kaons, while the prompt flux is produced in the decay of short-lived charmed hadrons [2]. Due to their longer lifetimes, pions and kaons are more likely to interact before decaying, resulting in a steeper energy spectrum. As a consequence, the conventional flux is expected to follow a power law with an index roughly one unit steeper than that of the primary cosmic rays, the latter being $\frac{d\phi}{dE} \propto E^{-2.7}$ [3–5]. This expectation was confirmed by earlier IceCube measurements, yielding the parametrization $\frac{d\phi}{dE} \propto E^{-3.78\pm0.02\ (\text{stat.})\pm0.03\ (\text{syst.})}$ [6].

The prompt flux arises from short-lived charmed hadrons that decay before interacting, producing a harder spectrum closer to the spectra of primary cosmic rays [7]. However, predicting the prompt component is more challenging, as its spectral shape and normalization are sensitive to the charm production models and the input cosmic ray spectrum. As discussed in [8], different astrophysical models can significantly influence the resulting spectral index of the prompt flux.

Astrophysical neutrinos originate from extragalactic sources. The astrophysical ν_μ flux is typically modeled with a single power-law spectrum. Several fits have been performed to describe this component, e.g. [2, 9–11], with the most recent measurement reporting a spectral index of $\gamma = -2.37\pm0.09$ [2].

Both the astrophysical neutrino flux and the prompt atmospheric component are expected to be angle-independent. The former because, without a horizon limiting their sources, astrophysical

neutrinos are expected to arrive uniformly from all directions, consistent with current observations [12]. The latter because prompt particles decay so rapidly that they are not affected by the column depth or interaction probability in the atmosphere, in contrast to the conventional flux component. The decay probability of muons is affected by the column depth of the atmosphere, which is zenith-dependent. At an incidence angle of 180°, the distance between the atmospheric origin of muons and the detector is maximised. At these steep angles, muons traverse longer paths through regions of lower air density, reducing their interaction rate and energy loss. Conversely, at smaller angles, muons pass through denser atmospheric layers, increasing the energy loss. This effect introduces an angular dependence in the energy spectrum of conventional muon neutrinos, as illustrated in Figure 1.

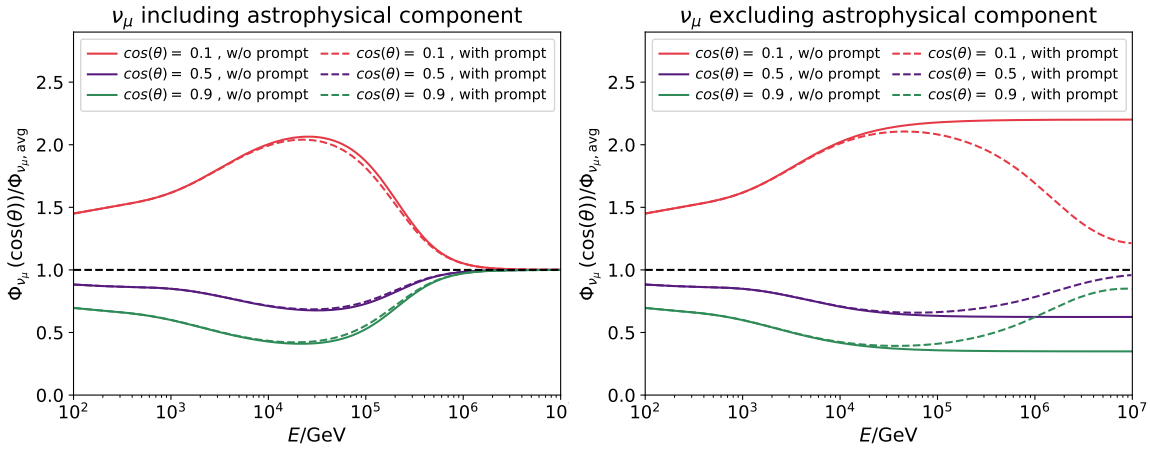

Figure 1: Relative energy spectra at cos(θ) = 0.1, 0.5 and 0.9 under different assumptions on the flux components, with astrophysical component (*left*) and without (*right*). Depicted are the conventional (*solid*) or conventional plus prompt (*dashed*) components.

3. Event Selection and Datasets

This analysis uses charged-current muon neutrino events from the Northern Hemisphere, where Earth shields atmospheric muon backgrounds. Muons produced in these interactions leave track-like signatures, as discussed in Section 1, which help distinguish them from other event types. The *HiveSplitter* algorithm [13] removes coincident events, and a decision tree classifier selects signal-like topologies with >90% probability and cascade rejection confidence above 0.5 [11]. Cascades are particle showers typically produced by neutral-current interactions of all neutrino flavors, or by charged-current interactions of electron and tau neutrinos, and they deposit their energy more locally in the detector. The final sample has 99.87% purity and $< 0.4°$ angular resolution [14], following standard IceCube procedures for diffuse sky analyses, such as [2, 15].

The resulting dataset spans a total of 11 years, covering the period from 2011 to 2021, which corresponds to an effective livetime of approximately 10.8 years in the IC86 configurations. With approximately 850,000 muon neutrino events detected. The neutrino energies in this sample range from 500 GeV to 4 PeV, with the lower threshold intentionally chosen to exclude the low-energy

region near the horizon, where the atmospheric muon background would be most severe [14]. The dataset covers zenith angles from 86° to 180° [11].

4. Spectrum Unfolding

The method used in this analysis is unfolding, as determining the energy spectrum of muon neutrinos constitutes an inverse problem. In IceCube and similar experiments, the true energy of the target particles is not measured directly. Instead, it is reconstructed from correlated observables. The relation between the neutrino and muon energy spectra is shown in Equation 1.

$$\frac{dN_\mu}{dE_\mu} = \int_{E_\mu}^{\infty} \left(\frac{dN_\nu}{dE_\nu}\right) \left(\frac{dP(E_\nu)}{dE_\mu}\right) dE_\nu, \tag{1}$$

The first term in the integral represents the neutrino spectrum, while the second describes the probability that a neutrino traveling through the detector produces a muon within it. This probability depends on the physics of neutrino interactions and muon propagation, and is independent of the specific form of the neutrino energy spectrum [5]. Consequently, the observed event distribution differs from the true distribution. Additional factors contributing to the difference between the measured and true distributions include detector effects, background contributions, and statistical fluctuations [16]. The background is omitted due to prior filtering (Section 3). To recover the true event distribution, the measured data must be corrected for the other effects, which are collectively encoded in the detector response matrix A. This procedure, known as unfolding, is governed by the *Fredholm integral equation*, as shown in Equation 2.

$$g(y) = \int_\Omega A(x, y) f(x)\, dx, \tag{2}$$

where $A(x, y)$ characterizes the detector response, $g(y)$ denotes the observed distribution in the proxy variable, and $f(x)$ represents the true distribution of the target quantity. In IceCube, the response matrix A is typically derived from Monte Carlo (MC) simulations. We discretize this relation as $\vec{g} = A_{m,n} \cdot \vec{f}$.

Monte Carlo (MC) simulations are employed to model the detector response and estimate the expected event distribution. These simulations are weighted according to theoretical neutrino flux models. The atmospheric flux is modeled with MCEq [17], using the SIBYLL2.3c hadronic interaction model [18] and the H3a model for cosmic ray composition [19]. The astrophysical component follows IceCube's diffuse 9.5-year astrophysical fit spectrum [2]. The weighted MC events are then used both to train the unfolding model and to construct the detector response matrix.

The *funfolding* library [20] was used, which applies MCMC-based optimization. Proxy and true energy values from MC are digitized, and a tree-based model maps $g(y)$ to $f(x)$ bins. Using these binned observable and true values, a linear unfolding model is constructed. The measured data, which contains only the reconstructed observables, is also binned using the previously trained model to form the $g(y)$ vector, and a likelihood with Tikhonov regularization (controlled by regularization strength tau, τ^{-1}) is minimized via MCMC [21, 22], yielding $f(x)$ and its uncertainties.

To quantify systematic uncertainties, such as those arising from ice properties or variations in DOM performance, the unfolding procedure was repeated multiple times using different systematic

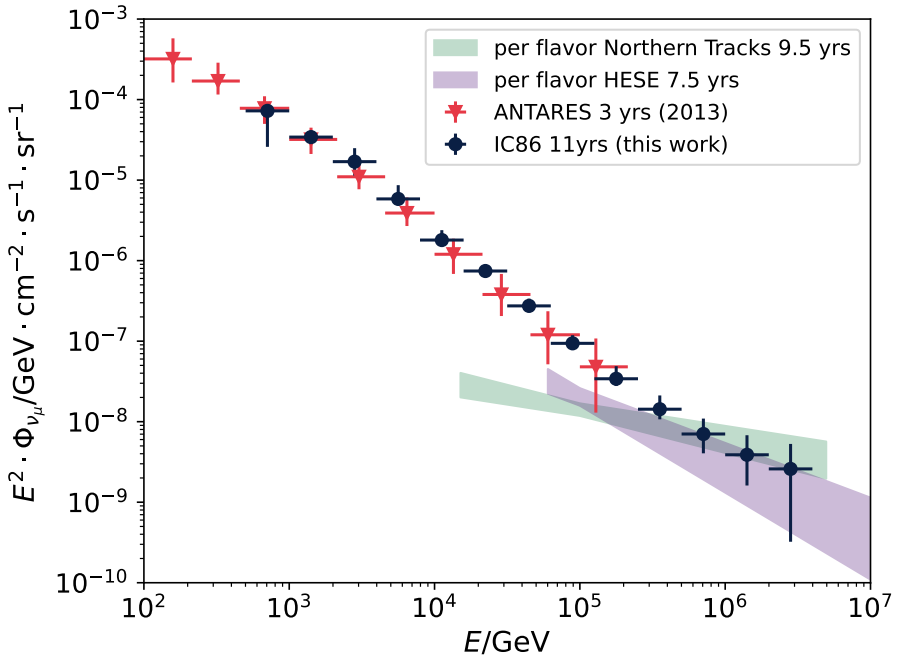

Figure 2: The measured energy spectrum (*black*) is compared with previous results from ANTARES (*red*) [23]. The astrophysical fits for the HESE analysis (*purple*) [24] and Diffuse Northern Tracks analysis (*green*) [2] are also displayed. Statistical and systematic uncertainties have been included.

parameter sets. In each set, one systematic parameter was shifted by a fixed amount while the others were held constant. The variations observed in the unfolded results due to these individual shifts were then used to estimate the corresponding systematic uncertainties.

5. Results

Using the methods described above, the unfolding result is depicted in Figure 2. The statistical and systematic uncertainties in the unfolded result are asymmetrical, as the flux values have been anchored to the points of highest probability within the range of systematic variations. For comparison, the unfolded spectrum from ANTARES from the 2013 through-going muon analysis have also been included [23], as well as the astrophysical flux fits from IceCube's 7.5-year HESE sample and the 9.5-year Northern Tracks sample [2, 24]. The unfolded IceCube spectrum shows good overall agreement within uncertainties with all three reference spectra across the relevant energy range. In particular, the consistency with the ANTARES result supports the compatibility of independent measurements using different detectors and reconstruction techniques at different timeframes. The error bands of the unfolded flux points overlap with both the HESE flux and the Northern Tracks 9.5-year fit, indicating broad consistency with previous IceCube measurements of the astrophysical neutrino flux within uncertainties.

Additionally, a comparison was made to a spectrum unfolding focusing on the seasonal dependence of muon neutrinos [25], using the same data set. This comparison is shown in Figure 3. The flux from the current analysis is shown in green, corresponding to a zenith range of 95° to 105°,

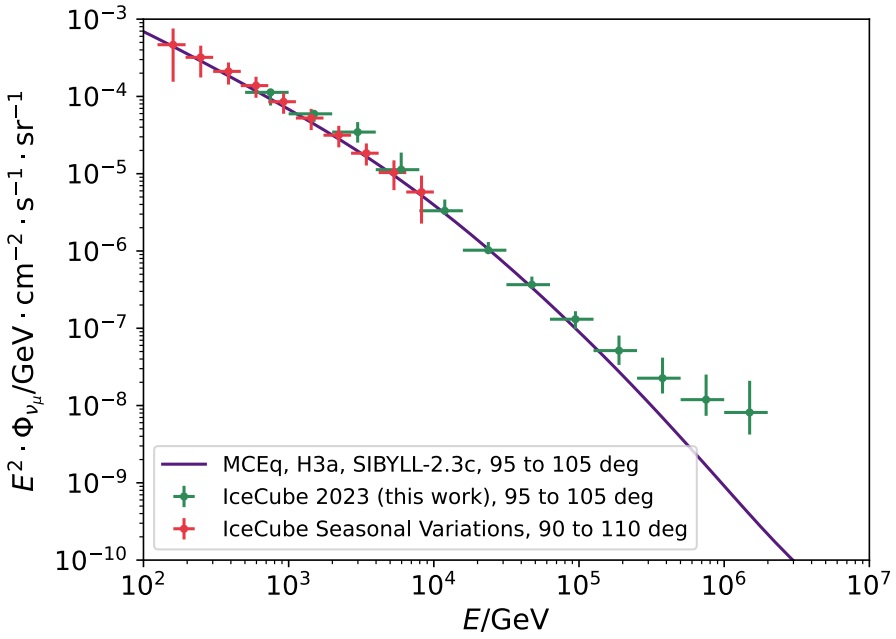

Figure 3: The muon neutrino flux from this work (*green*) compared to the flux from a recent analysis [25] in a similar angular range (*red*) and the atmospheric neutrino flux predicted by MCEq (*purple*) [17]. SIBILL-2.3c [18] was chosen as the hadronic interaction model and H3a to model the cosmic ray flux [19].

which was chosen to approximately match the range used in the seasonal analysis. The result from the seasonal study is shown in red, covering 90° to 110°. For reference, the theoretical expectation calculated using MCEq [17] is also shown in purple, evaluated at the same zenith range as this work. The two data sets agree reasonably well with each other and with the theoretical prediction.

At energies above 100 TeV, the unfolded flux from this work begins to systematically exceed the conventional atmospheric prediction from MCEq, suggesting the onset of an additional component. This excess is consistent with expectations for a diffuse astrophysical flux, which becomes increasingly dominant at high energies and is not accounted for in the purely atmospheric MCEq model. While statistical and systematic uncertainties in this region remain sizable, the observed trend aligns with previous IceCube observations of an astrophysical neutrino flux [2, 24], as shown in Figure 2, and is difficult to reconcile with a purely conventional atmospheric origin alone.

Dividing the eleven years of data into five zenith bins—86° to 95°, 95° to 105°, 105° to 117°, 117° to 134°, and 134° to 180°—and unfolding each bin separately results in Figure 4. Here, the ratio to the zenith-averaged flux is displayed for the five differently colored zenith bins, with continuous lines indicating the predicted theoretical flux by MCEq [17] for each respective bin.

At lower energies, zenith bands separate due to differences in atmospheric paths and meson decay probabilities: vertical directions yield a lower flux, while horizontal ones show a higher flux. Around 1 PeV, the different theoretical zenith bands converge. The obtained unfolding result also shows a level of convergence across zenith angles at high energies, similar to the behavior predicted by models that include an astrophysical component. In contrast, the purely conventional atmospheric flux shown in Figure 1 would be expected to maintain stronger angular separation.

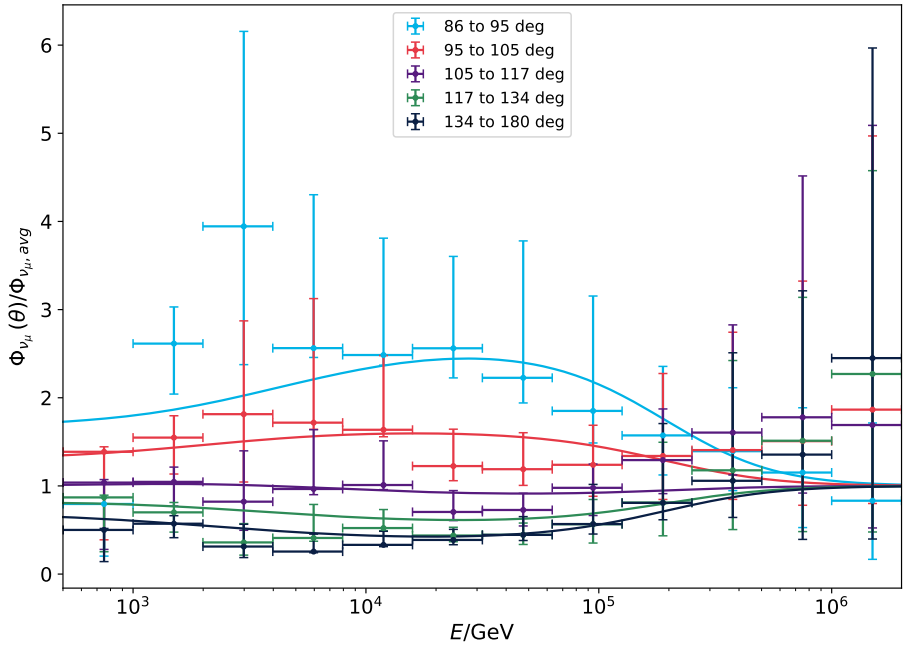

Figure 4: The Unfolded ratio of the different zenith bin ranges compared to the all range flux. The solid lines show the prediction of each particular zenith band computed by MCEq [17]. These bands were plotted using SIBYLL-2.3c [18] as an interaction model, the H3a model [19] for the primary cosmic ray flux, and the diffuse 9.5-year astrophysical fit [2]. The error bars depict the total uncertainty of the unfolding.

While this trend may suggest the presence of an additional, more isotropic component such as a diffuse astrophysical flux, the large uncertainties prevent any firm conclusions. In particular, the data do not allow for meaningful constraints on the presence of a prompt component or other effects from cosmic ray composition or hadronic interaction models.

6. Conclusion

In this analysis, the muon neutrino energy spectrum has been measured using 11 years of IceCube data. The event selection relied on well-reconstructed, up-going muon tracks from the Northern Hemisphere, ensuring high purity and angular resolution. By employing a machine-learning-based binning and Bayesian unfolding approach, the true energy distribution was extracted from reconstructed observables, accounting for detector effects and systematics.

The resulting spectrum is broadly consistent with previous IceCube measurements, showing agreement with the Northern Tracks characterization of the diffuse astrophysical neutrino flux [2] and remaining compatible with the HESE results [24] within the uncertainties. A previous measurement by the ANTARES collaboration using through-going muons [23] is in good agreement with the results presented here, with flux points that fall within each other's uncertainty bands. This consistency across different detectors and over a timescale of more than a decade reinforces the reliability of high-energy atmospheric neutrino measurements. A direct comparison with a recent IceCube muon neutrino spectrum obtained using a different unfolding algorithm shows good

agreement with respect to the systematic uncertainties within overlapping zenith ranges, supporting the robustness of the result.

By dividing the data into five zenith intervals, the angular dependence of the flux was studied in detail. The unfolded ratios indicate convergence with the angular average flux at high energies, consistent with the presence of an isotropic component. This behavior cannot be explained by a purely conventional atmospheric flux, as demonstrated in Section 2, and suggests that additional contributions, such as a diffuse astrophysical neutrino flux, are required to describe the data.

While this measurement does not allow conclusive statements about a prompt atmospheric component, it provides a high-statistics benchmark for future analyses. Improvements in systematic modeling and increased statistics at the highest energies will enable more detailed investigation of the transition between atmospheric and astrophysical neutrino contributions.

References

[1] **IceCube** Collaboration, N. N. Lad and D. Cowen, *PoS* **ICRC2023** (2023) 1122.

[2] **IceCube** Collaboration, R. Abbasi *et al.*, *The Astrophysical Journal* **928** no. 1, (2022) 50.

[3] **IceCube** Collaboration, R. Abbasi *et al.*, *Phys. Rev. D* **83** no. 1, (2011) 19.

[4] **IceCube** Collaboration, M. G. Aartsen *et al.*, *The European Physical Journal C* **75** no. 3, (2015) 116.

[5] T. Gaisser, *Cosmic Rays and Particle Physics*. Cambridge University Press, The Pitt Building, Trumpington Street, Cambridge CB2 1RP, 1990.

[6] **IceCube** Collaboration, M. Aartsen *et al.*, *Astroparticle Physics* **78** no. 1, (2016) 27.

[7] **IceCube** Collaboration, L. Kardum *et al.*, *PoS* **ICRC2023** (2023) 2307.14728.

[8] **IceCube** Collaboration, J. Böttcher *et al.*, *PoS* **ICRC2023** (2023) 2309.07560.

[9] **IceCube** Collaboration, J. Stettner *et al.*, *PoS* **ICRC2019** (2019) 1017.

[10] **IceCube** Collaboration, C. Haack, C. Wiebusch, *et al.*, *PoS* **ICRC2017** (2017) 301.

[11] **IceCube** Collaboration, M. G. Aartsen *et al.*, *The Astrophysical Journal* **833** no. 1, (2016) 3.

[12] **IceCube** Collaboration, M. Aartsen *et al.*, *The Astrophysical Journal* **849** no. 1, (2017) 67.

[13] **IceCube** Collaboration, M. Zoll *et al.*, *PoS* **ICRC2015** (2016) 1099.

[14] L. Kardum, *Unfolding the Muon Neutrino Flux*. Phd thesis, TU Dortmund, 2023. Available at https://eldorado.tu-dortmund.de/items/dfd11cd0-5280-469f-b624-763d8deb9b99.

[15] **IceCube** Collaboration, R. Abbasi *et al.*, *The European Physical Journal C* **83** no. 9, (2023) 777.

[16] S. Schmitt, *EPJ Web of Conferences* **137** (2017) 11008.

[17] A. Fedynitch, R. Engel, T. K. Gaisser, F. Riehn, and T. Stanev, *EPJ Web of Conferences* **99** (2015) 08001.

[18] F. Riehn, R. Engel, A. Fedynitch, T. K. Gaisser, T. Stanev, *et al.*, *PoS* **ICRC2015** (2015) 558.

[19] T. K. Gaisser, *Astroparticle Physics* **35** no. 12, (2012) 801–806.

[20] M. Börner, "funfolding: A flexible framework for unfolding problems in astroparticle physics." `https://github.com/tudo-astroparticlephysics/funfolding`, 2025. Accessed: 2025-05-22.

[21] D. P. O'Leary, *Linear Algebra and Its Applications* **31** no. 1, (1980) 111–134.

[22] D. van Ravenzwaaij, P. Cassey, and S. D. Brown, *Psychonomic Bulletin & Review* **25** no. 1, (2018) 143–154.

[23] **ANTARES** Collaboration, S. Adrián-Martínez *et al.*, *The European Physical Journal C* **73** no. 10, (2013) .

[24] **IceCube** Collaboration, R. Abbasi *et al.*, *Physical Review D* **104** no. 2, (2021) 57.

[25] **IceCube** Collaboration, R. Abbasi *et al.*, "Seasonal Variations of the Atmospheric Muon Neutrino Spectrum measured with IceCube," 2025. `https://arxiv.org/abs/2502.17890`.

Full Author List: IceCube Collaboration

R. Abbasi[16], M. Ackermann[63], J. Adams[17], S. K. Agarwalla[39, a], J. A. Aguilar[10], M. Ahlers[21], J.M. Alameddine[22], S. Ali[35], N. M. Amin[43], K. Andeen[41], C. Argüelles[13], Y. Ashida[52], S. Athanasiadou[63], S. N. Axani[43], R. Babu[23], X. Bai[49], J. Baines-Holmes[39], A. Balagopal V.[39, 43], S. W. Barwick[29], S. Bash[26], V. Basu[52], R. Bay[6], J. J. Beatty[19, 20], J. Becker Tjus[9, b], P. Behrens[1], J. Beise[61], C. Bellenghi[26], B. Benkel[63], S. BenZvi[51], D. Berley[18], E. Bernardini[47, c], D. Z. Besson[35], E. Blaufuss[18], L. Bloom[58], S. Blot[63], I. Bodo[39], F. Bontempo[30], J. Y. Book Motzkin[13], C. Boscolo Meneguolo[47, c], S. Böser[40], O. Botner[61], J. Böttcher[1], J. Braun[39], B. Brinson[4], Z. Brisson-Tsavoussis[32], R. T. Burley[2], D. Butterfield[39], M. A. Campana[48], K. Carloni[13], J. Carpio[33, 34], S. Chattopadhyay[39, a], N. Chau[10], Z. Chen[55], D. Chirkin[39], S. Choi[52], B. A. Clark[18], A. Coleman[61], P. Coleman[1], G. H. Collin[14], D. A. Coloma Borja[47], A. Connolly[19, 20], J. M. Conrad[14], R. Corley[52], D. F. Cowen[59, 60], C. De Clercq[11], J. J. DeLaunay[59], D. Delgado[13], T. Delmeulle[10], S. Deng[1], P. Desiati[39], K. D. de Vries[11], G. de Wasseige[36], T. DeYoung[23], J. C. Díaz-Vélez[39], S. DiKerby[23], M. Dittmer[42], A. Domi[25], L. Draper[52], L. Dueser[1], D. Durnford[24], K. Dutta[40], M. A. DuVernois[39], T. Ehrhardt[40], L. Eidenschink[26], A. Eimer[25], P. Eller[26], E. Ellinger[62], D. Elsässer[22], R. Engel[30, 31], H. Erpenbeck[39], W. Esmail[42], S. Eulig[13], J. Evans[18], P. A. Evenson[43], K. L. Fan[18], K. Fang[39], K. Farrag[15], A. R. Fazely[5], A. Fedynitch[57], N. Feigl[8], C. Finley[54], L. Fischer[63], D. Fox[59], A. Franckowiak[9], S. Fukami[63], P. Fürst[1], J. Gallagher[38], E. Ganster[1], A. Garcia[13], M. Garcia[43], G. Garg[39, a], E. Genton[13, 36], L. Gerhardt[7], A. Ghadimi[58], C. Glaser[61], T. Glüsenkamp[61], J. G. Gonzalez[43], S. Goswami[33, 34], A. Granados[23], D. Grant[12], S. J. Gray[18], S. Griffin[39], S. Griswold[51], K. M. Groth[21], D. Guevel[39], C. Günther[1], P. Gutjahr[22], C. Ha[53], C. Haack[25], A. Hallgren[61], L. Halve[1], F. Halzen[39], L. Hamacher[1], M. Ha Minh[26], M. Handt[1], K. Hanson[39], J. Hardin[14], A. A. Harnisch[23], P. Hatch[32], A. Haungs[30], J. Häußler[1], K. Helbing[62], J. Hellrung[9], B. Henke[23], L. Hennig[25], F. Henningsen[12], L. Heuermann[1], R. Hewett[17], N. Heyer[61], S. Hickford[62], A. Hidvegi[54], C. Hill[15], G. C. Hill[2], R. Hmaid[15], K. D. Hoffman[18], D. Hooper[39], S. Hori[39], K. Hoshina[39, d], M. Hostert[13], W. Hou[30], T. Huber[30], K. Hultqvist[54], K. Hymon[22, 57], A. Ishihara[15], W. Iwakiri[15], M. Jacquart[21], S. Jain[39], O. Janik[25], M. Jansson[36], M. Jeong[52], M. Jin[13], N. Kamp[13], D. Kang[30], W. Kang[48], X. Kang[48], A. Kappes[42], L. Kardum[22], T. Karg[63], M. Karl[26], A. Karle[39], A. Katil[24], M. Kauer[39], J. L. Kelley[39], M. Khanal[52], A. Khatee Zathul[39], A. Kheirandish[33, 34], H. Kimku[53], J. Kiryluk[55], C. Klein[25], S. R. Klein[6, 7], Y. Kobayashi[15], A. Kochocki[23], R. Koirala[43], H. Kolanoski[8], T. Kontrimas[26], L. Köpke[40], C. Kopper[25], D. J. Koskinen[21], P. Koundal[43], M. Kowalski[8, 63], T. Kozynets[21], N. Krieger[9], J. Krishnamoorthi[39, a], T. Krishnan[13], K. Kruiswijk[36], E. Krupczak[23], A. Kumar[63], E. Kun[9], N. Kurahashi[48], N. Lad[63], C. Lagunas Gualda[26], L. Lallement Arnaud[10], M. Lamoureux[36], M. J. Larson[18], F. Lauber[62], J. P. Lazar[36], K. Leonard DeHolton[60], A. Leszczyńska[43], J. Liao[4], C. Lin[43], Y. T. Liu[60], M. Liubarska[24], C. Love[48], L. Lu[39], F. Lucarelli[27], W. Luszczak[19, 20], Y. Lyu[6, 7], J. Madsen[39], E. Magnus[11], K. B. M. Mahn[23], Y. Makino[39], E. Manao[26], S. Mancina[47, e], A. Mand[39], I. C. Mariş[10], S. Marka[45], Z. Marka[45], L. Marten[1], I. Martinez-Soler[13], R. Maruyama[44], J. Mauro[36], F. Mayhew[23], F. McNally[37], J. V. Mead[21], K. Meagher[39], S. Mechbal[63], A. Medina[20], M. Meier[15], Y. Merckx[11], L. Merten[9], J. Mitchell[5], L. Molchany[49], T. Montaruli[27], R. W. Moore[24], Y. Morii[15], A. Mosbrugger[25], M. Moulai[39], D. Mousadi[63], E. Moyaux[36], T. Mukherjee[30], R. Naab[63], M. Nakos[39], U. Naumann[62], J. Necker[63], L. Neste[54], M. Neumann[42], H. Niederhausen[23], M. U. Nisa[23], K. Noda[15], A. Noell[1], A. Novikov[43], A. Obertacke Pollmann[15], V. O'Dell[39], A. Olivas[18], R. Orsoe[26], J. Osborn[39], E. O'Sullivan[61], V. Palusova[40], H. Pandya[43], A. Parenti[10], N. Park[32], V. Parrish[23], E. N. Paudel[58], L. Paul[49], C. Pérez de los Heros[61], T. Pernice[63], J. Peterson[39], M. Plum[49], A. Pontén[61], V. Poojyam[58], Y. Popovych[40], M. Prado Rodriguez[39], B. Pries[23], R. Procter-Murphy[18], G. T. Przybylski[7], L. Pyras[52], C. Raab[36], J. Rack-Helleis[40], N. Rad[63], M. Ravn[61], K. Rawlins[3], Z. Rechav[39], A. Rehman[43], I. Reistroffer[49], E. Resconi[26], S. Reusch[63], C. D. Rho[56], W. Rhode[22], L. Ricca[36], B. Riedel[39], A. Rifaie[62], E. J. Roberts[2], S. Robertson[6, 7], M. Rongen[25], A. Rosted[15], C. Rott[52], T. Ruhe[22], L. Ruohan[26], D. Ryckbosch[28], J. Saffer[31], D. Salazar-Gallegos[23], P. Sampathkumar[30], A. Sandrock[62], G. Sanger-Johnson[23], M. Santander[58], S. Sarkar[46], J. Savelberg[1], M. Scarnera[36], P. Schaile[26], M. Schaufel[1], H. Schieler[30], S. Schindler[25], L. Schlickmann[40], B. Schlüter[42], F. Schlüter[10], N. Schmeisser[62], T. Schmidt[18], F. G. Schröder[30, 43], L. Schumacher[25], S. Schwirn[1], S. Sclafani[18], D. Seckel[43], L. Seen[39], M. Seikh[35], S. Seunarine[50], P. A. Sevle Myhr[36], R. Shah[48], S. Shefali[31], N. Shimizu[15], B. Skrzypek[6], R. Snihur[39], J. Soedingrekso[22], A. Søgaard[21], D. Soldin[52], P. Soldin[1], G. Sommani[9], C. Spannfellner[26], G. M. Spiczak[50], C. Spiering[63], J. Stachurska[28], M. Stamatikos[20], T. Stanev[43], T. Stezelberger[7], T. Stürwald[62], T. Stuttard[21], G. W. Sullivan[18], I. Taboada[4], S. Ter-Antonyan[5], A. Terliuk[26], A. Thakuri[49], M. Thiesmeyer[39], W. G. Thompson[13], J. Thwaites[39], S. Tilav[43], K. Tollefson[23], S. Toscano[10], D. Tosi[39], A. Trettin[63], A. K. Upadhyay[39, a], K. Upshaw[5], A. Vaidyanathan[41], N. Valtonen-Mattila[9, 61], J. Valverde[41], J. Vandenbroucke[39], T. van Eeden[63], N. van Eijndhoven[11], L. van Rootselaar[22], J. van Santen[63], F. J. Vara Carbonell[42], F. Varsi[31], M. Venugopal[30], M. Vereecken[36], S. Vergara Carrasco[17], S. Verpoest[43], D. Veske[45], A. Vijai[18], J. Villarreal[14], C. Walck[54], A. Wang[4], E. Warrick[58], C. Weaver[23], P. Weigel[14], A. Weindl[30], J. Weldert[40], A. Y. Wen[13], C. Wendt[39], J. Werthebach[22], M. Weyrauch[30], N. Whitehorn[23], C. H. Wiebusch[1], D. R. Williams[58], L. Witthaus[22], M. Wolf[26], G. Wrede[25], X. W. Xu[5], J. P. Yañez[24], Y. Yao[39], E. Yildizci[39], S. Yoshida[15], R. Young[35], F. Yu[13], S. Yu[52], T. Yuan[39], A. Zegarelli[9], S. Zhang[23], Z. Zhang[55], P. Zhelnin[13], P. Zilberman[39]

[1] III. Physikalisches Institut, RWTH Aachen University, D-52056 Aachen, Germany
[2] Department of Physics, University of Adelaide, Adelaide, 5005, Australia
[3] Dept. of Physics and Astronomy, University of Alaska Anchorage, 3211 Providence Dr., Anchorage, AK 99508, USA
[4] School of Physics and Center for Relativistic Astrophysics, Georgia Institute of Technology, Atlanta, GA 30332, USA
[5] Dept. of Physics, Southern University, Baton Rouge, LA 70813, USA
[6] Dept. of Physics, University of California, Berkeley, CA 94720, USA
[7] Lawrence Berkeley National Laboratory, Berkeley, CA 94720, USA
[8] Institut für Physik, Humboldt-Universität zu Berlin, D-12489 Berlin, Germany
[9] Fakultät für Physik & Astronomie, Ruhr-Universität Bochum, D-44780 Bochum, Germany
[10] Université Libre de Bruxelles, Science Faculty CP230, B-1050 Brussels, Belgium

[11] Vrije Universiteit Brussel (VUB), Dienst ELEM, B-1050 Brussels, Belgium
[12] Dept. of Physics, Simon Fraser University, Burnaby, BC V5A 1S6, Canada
[13] Department of Physics and Laboratory for Particle Physics and Cosmology, Harvard University, Cambridge, MA 02138, USA
[14] Dept. of Physics, Massachusetts Institute of Technology, Cambridge, MA 02139, USA
[15] Dept. of Physics and The International Center for Hadron Astrophysics, Chiba University, Chiba 263-8522, Japan
[16] Department of Physics, Loyola University Chicago, Chicago, IL 60660, USA
[17] Dept. of Physics and Astronomy, University of Canterbury, Private Bag 4800, Christchurch, New Zealand
[18] Dept. of Physics, University of Maryland, College Park, MD 20742, USA
[19] Dept. of Astronomy, Ohio State University, Columbus, OH 43210, USA
[20] Dept. of Physics and Center for Cosmology and Astro-Particle Physics, Ohio State University, Columbus, OH 43210, USA
[21] Niels Bohr Institute, University of Copenhagen, DK-2100 Copenhagen, Denmark
[22] Dept. of Physics, TU Dortmund University, D-44221 Dortmund, Germany
[23] Dept. of Physics and Astronomy, Michigan State University, East Lansing, MI 48824, USA
[24] Dept. of Physics, University of Alberta, Edmonton, Alberta, T6G 2E1, Canada
[25] Erlangen Centre for Astroparticle Physics, Friedrich-Alexander-Universität Erlangen-Nürnberg, D-91058 Erlangen, Germany
[26] Physik-department, Technische Universität München, D-85748 Garching, Germany
[27] Département de physique nucléaire et corpusculaire, Université de Genève, CH-1211 Genève, Switzerland
[28] Dept. of Physics and Astronomy, University of Gent, B-9000 Gent, Belgium
[29] Dept. of Physics and Astronomy, University of California, Irvine, CA 92697, USA
[30] Karlsruhe Institute of Technology, Institute for Astroparticle Physics, D-76021 Karlsruhe, Germany
[31] Karlsruhe Institute of Technology, Institute of Experimental Particle Physics, D-76021 Karlsruhe, Germany
[32] Dept. of Physics, Engineering Physics, and Astronomy, Queen's University, Kingston, ON K7L 3N6, Canada
[33] Department of Physics & Astronomy, University of Nevada, Las Vegas, NV 89154, USA
[34] Nevada Center for Astrophysics, University of Nevada, Las Vegas, NV 89154, USA
[35] Dept. of Physics and Astronomy, University of Kansas, Lawrence, KS 66045, USA
[36] Centre for Cosmology, Particle Physics and Phenomenology - CP3, Université catholique de Louvain, Louvain-la-Neuve, Belgium
[37] Department of Physics, Mercer University, Macon, GA 31207-0001, USA
[38] Dept. of Astronomy, University of Wisconsin—Madison, Madison, WI 53706, USA
[39] Dept. of Physics and Wisconsin IceCube Particle Astrophysics Center, University of Wisconsin—Madison, Madison, WI 53706, USA
[40] Institute of Physics, University of Mainz, Staudinger Weg 7, D-55099 Mainz, Germany
[41] Department of Physics, Marquette University, Milwaukee, WI 53201, USA
[42] Institut für Kernphysik, Universität Münster, D-48149 Münster, Germany
[43] Bartol Research Institute and Dept. of Physics and Astronomy, University of Delaware, Newark, DE 19716, USA
[44] Dept. of Physics, Yale University, New Haven, CT 06520, USA
[45] Columbia Astrophysics and Nevis Laboratories, Columbia University, New York, NY 10027, USA
[46] Dept. of Physics, University of Oxford, Parks Road, Oxford OX1 3PU, United Kingdom
[47] Dipartimento di Fisica e Astronomia Galileo Galilei, Università Degli Studi di Padova, I-35122 Padova PD, Italy
[48] Dept. of Physics, Drexel University, 3141 Chestnut Street, Philadelphia, PA 19104, USA
[49] Physics Department, South Dakota School of Mines and Technology, Rapid City, SD 57701, USA
[50] Dept. of Physics, University of Wisconsin, River Falls, WI 54022, USA
[51] Dept. of Physics and Astronomy, University of Rochester, Rochester, NY 14627, USA
[52] Department of Physics and Astronomy, University of Utah, Salt Lake City, UT 84112, USA
[53] Dept. of Physics, Chung-Ang University, Seoul 06974, Republic of Korea
[54] Oskar Klein Centre and Dept. of Physics, Stockholm University, SE-10691 Stockholm, Sweden
[55] Dept. of Physics and Astronomy, Stony Brook University, Stony Brook, NY 11794-3800, USA
[56] Dept. of Physics, Sungkyunkwan University, Suwon 16419, Republic of Korea
[57] Institute of Physics, Academia Sinica, Taipei, 11529, Taiwan
[58] Dept. of Physics and Astronomy, University of Alabama, Tuscaloosa, AL 35487, USA
[59] Dept. of Astronomy and Astrophysics, Pennsylvania State University, University Park, PA 16802, USA
[60] Dept. of Physics, Pennsylvania State University, University Park, PA 16802, USA
[61] Dept. of Physics and Astronomy, Uppsala University, Box 516, SE-75120 Uppsala, Sweden
[62] Dept. of Physics, University of Wuppertal, D-42119 Wuppertal, Germany
[63] Deutsches Elektronen-Synchrotron DESY, Platanenallee 6, D-15738 Zeuthen, Germany
[a] also at Institute of Physics, Sachivalaya Marg, Sainik School Post, Bhubaneswar 751005, India
[b] also at Department of Space, Earth and Environment, Chalmers University of Technology, 412 96 Gothenburg, Sweden
[c] also at INFN Padova, I-35131 Padova, Italy
[d] also at Earthquake Research Institute, University of Tokyo, Bunkyo, Tokyo 113-0032, Japan
[e] now at INFN Padova, I-35131 Padova, Italy

PoS(ICRC2025)1199

Acknowledgments

The authors gratefully acknowledge the support from the following agencies and institutions: USA – U.S. National Science Foundation-Office of Polar Programs, U.S. National Science Foundation-Physics Division, U.S. National Science Foundation-EPSCoR, U.S. National Science Foundation-Office of Advanced Cyberinfrastructure, Wisconsin Alumni Research Foundation, Center for High Throughput Computing (CHTC) at the University of Wisconsin–Madison, Open Science Grid (OSG), Partnership to Advance Throughput Computing (PATh), Advanced Cyberinfrastructure Coordination Ecosystem: Services & Support (ACCESS), Frontera and Ranch computing project at the Texas Advanced Computing Center, U.S. Department of Energy-National Energy Research Scientific Computing Center, Particle astrophysics research computing center at the University of Maryland, Institute for Cyber-Enabled Research at Michigan State University, Astroparticle physics computational facility at Marquette University, NVIDIA Corporation, and Google Cloud Platform; Belgium – Funds for Scientific Research (FRS-FNRS and FWO), FWO Odysseus and Big Science programmes, and Belgian Federal Science Policy Office (Belspo); Germany – Bundesministerium für Forschung, Technologie und Raumfahrt (BMFTR), Deutsche Forschungsgemeinschaft (DFG), Helmholtz Alliance for Astroparticle Physics (HAP), Initiative and Networking Fund of the Helmholtz Association, Deutsches Elektronen Synchrotron (DESY), and High Performance Computing cluster of the RWTH Aachen; Sweden – Swedish Research Council, Swedish Polar Research Secretariat, Swedish National Infrastructure for Computing (SNIC), and Knut and Alice Wallenberg Foundation; European Union – EGI Advanced Computing for research; Australia – Australian Research Council; Canada – Natural Sciences and Engineering Research Council of Canada, Calcul Québec, Compute Ontario, Canada Foundation for Innovation, WestGrid, and Digital Research Alliance of Canada; Denmark – Villum Fonden, Carlsberg Foundation, and European Commission; New Zealand – Marsden Fund; Japan – Japan Society for Promotion of Science (JSPS) and Institute for Global Prominent Research (IGPR) of Chiba University; Korea – National Research Foundation of Korea (NRF); Switzerland – Swiss National Science Foundation (SNSF).